Osteoblast expression of an engineered G_s-coupled receptor dramatically increases bone mass

Edward C. Hsiao[†‡§], Benjamin M. Boudignon[¶], Wei C. Chang[†‖], Margaret Bencsik[¶], Jeffrey Peng[¶], Trieu D. Nguyen[†], Carlota Manalac[†], Bernard P. Halloran[‡¶], Bruce R. Conklin[†‡§††], and Robert A. Nissenson[‡§¶]

[†]Gladstone Institute of Cardiovascular Disease, San Francisco, CA 94158; [‡]Department of Medicine, University of California, San Francisco, CA 94143; [¶]Endocrine Research Unit, Veterans Affairs Medical Center and Departments of Medicine and Physiology, University of California, San Francisco, CA 94121; [‖]Graduate Program in Pharmaceutical Sciences and Pharmacogenomics, University of California, San Francisco, CA 94158; and [††]Department of Cellular and Molecular Pharmacology, University of California, San Francisco, CA 94158

Edited by Kathryn V. Anderson, Sloan–Kettering Institute, New York, NY, and approved November 28, 2007 (received for review August 7, 2007)

Osteoblasts are essential for maintaining bone mass, avoiding osteoporosis, and repairing injured bone. Activation of osteoblast G protein-coupled receptors (GPCRs), such as the parathyroid hormone receptor, can increase bone mass; however, the anabolic mechanisms are poorly understood. Here we use "Rs1," an engineered GPCR with constitutive G_s signaling, to evaluate the temporal and skeletal effects of G_s signaling in murine osteoblasts. *In vivo*, Rs1 expression induces a dramatic anabolic skeletal response, with midfemur girth increasing 1,200% and femur mass increasing 380% in 9-week-old mice. Bone volume, cellularity, areal bone mineral density, osteoblast gene markers, and serum bone turnover markers were also elevated. No such phenotype developed when Rs1 was expressed after the first 4 weeks of postnatal life, indicating an exquisite temporal sensitivity of osteoblasts to Rs1 expression. This pathway may represent an important determinant of bone mass and may open future avenues for enhancing bone repair and treating metabolic bone diseases.

RASSL | constitutive G_s activity | bone formation | cyclic AMP | McCune–Albright syndrome

Cells from the osteoblast lineage play key roles in the regulation of bone development, acquisition of peak bone mass, maintenance and repair of the adult skeleton, and calcium homeostasis (1). Osteoblast dysfunction leading to bone loss is thought to be a key mechanism in osteoporosis, which affects >10 million people in the United States and contributes to 1.5 million fractures each year (2). Bone fractures constitute >3 million emergency department visits a year in the United States (3). Although activation of osteoblast G protein-coupled receptors (GPCRs), such as the parathyroid hormone receptor (PTHR1) by recombinant PTH (1–34) (teriparatide), can increase bone mass (4), the exact *in vivo* roles of the various G protein signaling pathways, and how they interact with other aspects of skeletal biology, have not been clearly elucidated.

GPCRs signal through a select number of pathways, including the G_s and G_i pathways that influence intracellular cAMP levels (5). Human genetic diseases involving the $G_s\alpha$ subunit (*GNAS*) suggest that G_s signaling can influence bone growth (6). Inactivation of *GNAS* in humans leads to multiple endocrinopathies and short stature from rapid growth plate maturation, as seen in Albright's hereditary osteodystrophy (AHO; Online Mendelian Inheritance in Man no. 103580). Mouse models of AHO with chondrocyte- or osteoblast-specific inactivation of *GNAS* show severe alterations in chondrocyte maturation (7) or cortical bone formation (8), respectively.

In contrast, abnormal genetic activation of *GNAS* in humans leads to McCune–Albright syndrome (MAS; Online Mendelian Inheritance in Man no. 174800), which is characterized by alterations in bone and cartilage formation as well as multiple types of endocrine tumors (9). Mice expressing a constitutively active PTHR1 in osteoblasts show increased trabecular bone volume and decreased cortical bone thickness at 12 weeks of age, with grossly normal femur shape and size (10, 11). In addition, models using PTH peptide fragments that selectively activate PTHR1-linked G_s signaling (12–15) suggest that G_s signaling can increase bone formation. Because a mouse model with constitutively active *GNAS* in osteoblasts has not been developed, the direct role of activated G_s signaling in osteoblasts has not been clearly tested.

We sought to create a system that would permit selective and reversible activation of a single G protein-linked pathway in a tissue-specific manner. Receptors activated solely by a synthetic ligand (RASSLs) provide one method for experimentally manipulating the timing and signaling of G protein pathways (16, 17). RASSLs are engineered receptors that no longer respond to endogenous hormones but can be activated by synthetic small-molecule drugs. They have proven useful for studying the roles of activated G protein signaling (18–20) and basal G protein activity (21, 22) in complex systems, including cardiomyocyte and neurological development and function.

The human 5HT4b serotonin receptor is strongly associated with G_s activity and displays high basal signaling that is ideal for constitutively activating the G_s pathway. In addition, the large number of pharmacologic agents active on 5HT4 receptors makes this receptor class an ideal substrate for creating RASSLs. Here we use a unique G_s-coupled RASSL, Rs1, with constitutive G_s signaling activity to examine the temporal and skeletal effects of G_s signaling in murine osteoblasts.

Results

To generate Rs1 [Fig. 1*A*, and see supporting information (SI) Fig. 5*A*] with pharmacological responses similar to those of the murine 5HT4-D100A RASSL (23), we introduced the corresponding D100A mutation and a FLAG tag into the human 5HT4b receptor. *In vitro* analysis of Rs1 function by transient transfection in HEK293 cells demonstrated that Rs1 had robust basal signaling that increased intracellular cAMP (Fig. 1*B*), with no detectable G_q-linked basal signaling (SI Fig. 5*B*). Because Rs1

Author contributions: E.C.H., B.M.B., W.C.C., B.P.H., B.R.C., and R.A.N. designed research; E.C.H., B.M.B., W.C.C., M.B., J.P., T.D.N., C.M., B.P.H., B.R.C., and R.A.N. performed research; M.B. contributed new reagents/analytic tools; E.C.H., B.M.B., W.C.C., B.P.H., B.R.C., and R.A.N. analyzed data; and E.C.H., B.R.C., and R.A.N. wrote the paper.

The authors declare no conflict of interest.

This article is a PNAS Direct Submission.

Freely available online through the PNAS open access option.

Data deposition: The mouse strains reported in this paper have been deposited in the Mutant Mouse Regional Resource Centers (MMRRC) database [accession nos. 029992 FVB/N-Tg(TetO-HTR4*D100A) (TetO-Rs1-line G) and 029993 FVB/N-Tg(TetO-HTR4*D100A) (TetO-Rs1-line B)]. The plasmids reported in this paper have been deposited in the Addgene database [accession nos. 16313 (pUHG10.3 TetO-Rs1) and 16312 (pUNIV-SIG-5HT4D100A)].

[§]To whom correspondence may be addressed. E-mail: ehsiao@gladstone.ucsf.edu, bconklin@gladstone.ucsf.edu, or robert.nissenson@va.gov.

This article contains supporting information online at www.pnas.org/cgi/content/full/0707457105/DC1.

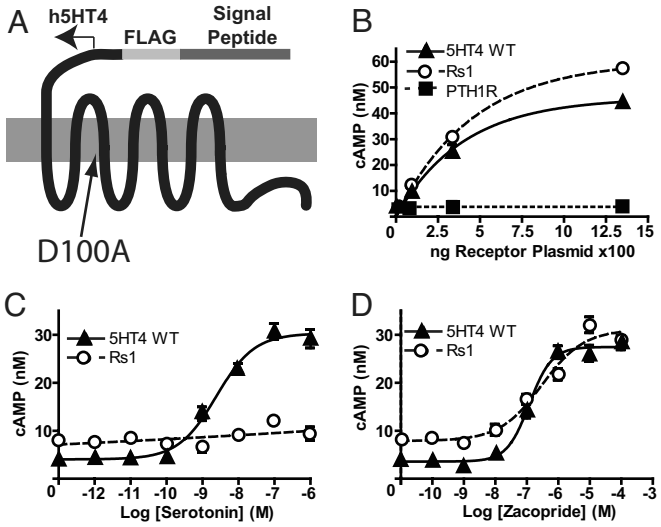

Fig. 1. Characteristics of the G_s-coupled RASSL Rs1. (*A*) Rs1 was generated by introducing a D100A mutation into the human 5HT4b serotonin receptor and adding an N-terminal FLAG tag. The amino acid sequence is shown in SI Fig. 5*A*. (*B*) Basal cAMP mobilization in HEK293 cells transfected with increasing amounts of Rs1 plasmid DNA demonstrated high levels of Rs1 basal activity, in contrast to receptors having low basal activity [e.g., WT murine parathyroid hormone receptor (PTHR1)]. (*C*) Rs1 receptor plasmid DNA (25 ng) electroporated into HEK293 cells initiates a minimal increase in cAMP in response to the endogenous 5HT4 ligand, serotonin. (*D*) Rs1 mobilized cAMP to the same degree as WT 5HT4b receptor when stimulated with the synthetic 5HT4 receptor agonist, zacopride. *B–D* show representative data from independent experiments repeated three times for each condition. Error bars (which may be obscured by the data point symbol) represent ±1 SD from technical triplicates.

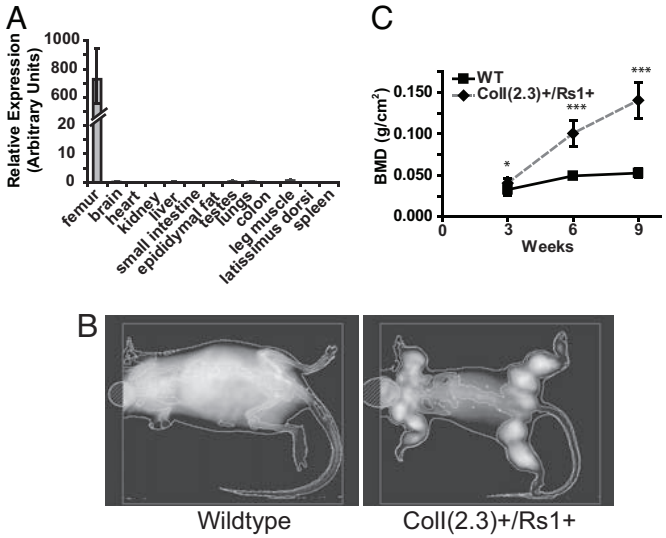

Fig. 2. Effects of osteoblast expression of Rs1, a receptor with constitutive G_s signaling activity. (*A*) Bone-specific expression of Rs1, using the tTA (TetOff) system in ColI(2.3)+/Rs1+ mice conceived and maintained off of doxycycline, was confirmed by qPCR. A representative adult mouse is shown, with similar expression profiles seen in three independent animals. Error bars represent ±1 SD for technical triplicates per tissue. (*B*) DEXA images show enhanced mineral accrual in the bones of 9-week-old double transgenic mice (*Right*) and littermate controls (*Left*). (*C*) BMD measured in age-matched littermates at 3 (n = 10 WT, 14 mutant), 6 (n = 10 WT, 10 mutant), and 9 (n = 8 WT, 14 mutant) weeks showed continued progression of the phenotype. No differences were noted between male and female mice or between single transgenic mice and WT mice (SI Fig. 6). Error bars represent ±1 SD. *, $P < 0.05$; ***, $P < 0.0005$ by t test of Rs1-expressing mice vs. control genotypes.

does not respond to serotonin (Fig. 1*C*), the magnitude of G_s-mediated signaling by Rs1 should depend solely on the level of Rs1 expression and not on endogenous serotonin levels, which we cannot control. Rs1 retained agonist-dependent increases in cAMP production in response to several synthetic 5HT4 receptor agonists, including zacopride (Fig. 1*D*), demonstrating that the receptor is folded properly, inserted into the plasma membrane, and capable of signaling through the native G_s pathway.

Because G_s activity is crucial in a variety of tissues, we used the tetracycline transactivator (tTA) system ("TetOff") (24, 25) to provide temporal control of Rs1 expression (SI Fig. 5*C*). To obtain spatial control, TetO-Rs1 transgenic mice were mated with transgenic mice expressing tTA under the control of the osteoblast-specific Col1α-1 2.3-kb promoter fragment (26). In the absence of doxycycline, double transgenic progeny [designated ColI(2.3)+/Rs1+] expressed high levels of Rs1 in whole femurs but not in nonskeletal tissues, as assayed by quantitative real-time PCR (qPCR) (Fig. 2*A*). These results are consistent with published descriptions of the Col1α-1 2.3-kb promoter fragment being active in maturing osteoblasts (27, 28). Little or no Rs1 expression was detected in skeletal tissue from ColI(2.3)+/Rs1+ mice maintained on doxycycline or in skeletal tissue from TetO-Rs1 single transgenic mice (SI Fig. 5*D*).

Because of the high level of Rs1 transgene expression in ColI(2.3)+/Rs1+ mice, we hypothesized that basal Rs1 signaling activity might be sufficient to alter bone mass *in vivo*. ColI(2.3)+/Rs1+ mice that were maintained off of doxycycline from conception were phenotypically indistinguishable from littermate controls at birth but displayed notable asymmetric enlargement of the skeleton starting at 3 weeks of age. These characteristics became more pronounced and generalized as the mice aged. Although body weights (SI Fig. 6 *A* and *B*) for all mice remained similar through 9 weeks of age, double transgenic mice were shorter than their single transgenic and wild-type (WT) littermate controls starting at 6 weeks of age (SI Fig. 6 *C* and *D*).

As determined by dual-energy x-ray absorptiometry (DEXA) scanning, ColI(2.3)+/Rs1+ mice displayed an osteosclerotic phenotype with increased bone mineral (Fig. 2*B*). At 9 weeks of age, both female (SI Fig. 6*E*) and male (SI Fig. 6*F*) mice showed dramatic increases (380%) in whole-body areal bone mineral density (BMD) (Fig. 2*C*). No significant differences were observed in BMD, weight, or length within the littermate control genotypes [ColI(2.3)+ or Rs1+ single transgenics and wild types] or between males and females. In addition, three distinct TetO-Rs1 responder transgenic mouse lines gave similar results, confirming that the bony changes were not due to transgene integration effects. ColI(2.3)+/Rs1+ mice maintained off of doxycycline continued to show progression of the bone phenotype, requiring euthanasia by 30 weeks of age from complications of spinal stenosis, infection, or failure to thrive. Mice maintained on doxycycline from conception did not develop the bone phenotype.

A more detailed characterization of the bony lesions was obtained by microCT analysis (Fig. 3 *A–C*). The bones of ColI(2.3)+/Rs1+ newborn mice were normal in structure, location, and size, indicating grossly normal developmental patterning. Whole-skeleton alizarin red staining confirmed normal development of the craniofacial structures, with normal tooth eruption (data not shown). At 3 weeks of age, a moderate increase in femur size and an increase in bone accrual within the skull were evident in ColI(2.3)+/Rs1+ mice. High-resolution CT scans of femurs from 3-week-old mice showed a significant replacement of the normal long bone structures within the diaphysis by disorganized trabecular bone (Fig. 3 *D* and *E*). The joints and primary spongiosa appeared to be spared from the increased bone formation (SI Movie 1). Morphometric

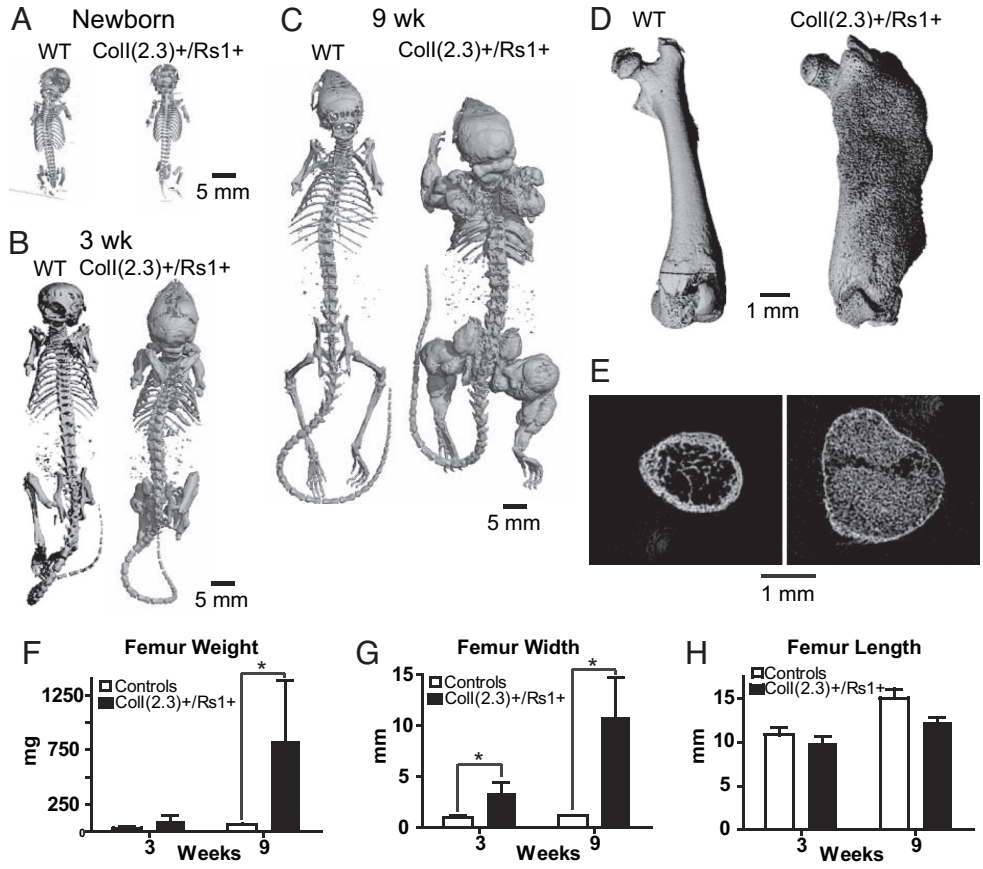

Fig. 3. Skeletal effects of osteoblast expression of Rs1 by microCT. (*A–C*) Whole-body CT analysis of ColI(2.3)+/Rs1+ mice and WT littermate controls (50-μm resolution) shows dramatically enhanced bone accumulation in double transgenic mice that progresses with age. (*D*) Femurs from WT and double transgenic mice, illustrating the increase in bone width and effacement of cortical bone produced by Rs1 expression. Note that the articular surfaces of the bones appear minimally affected. (*E*) Cross-sectional CT images (10-μm resolution) of femurs from WT (*Left*) and ColI(2.3)+/Rs1+ (*Right*) mice show a predominance of trabecular bone with effacement of the cortical shell in double transgenic mice. (*F–H*) Double transgenic mice display increased femur weight (*F*) and width (*G*), but not length (*H*). $n = 4$ WT and 4 mutants at 3 weeks; $n = 2$ WT and 5 mutants at 9 weeks. Error bars represent ± 1 SD. *, $P < 0.05$ by *t* test of Rs1-expressing mice vs. WT controls.

measurements of femurs from 3-week-old mice showed large increases in femur weight and mid-diaphyseal diameter but not femur length (Fig. 3 *F–H*). The fine trabecular structure of the abnormal bone in the ColI(2.3)+/Rs1+ mice limited our ability to accurately determine segmented bone density. By 9 weeks of age, significant and generalized bony lesions were noted in all ColI(2.3)+/Rs1+ mice (SI Movie 2). No heterotopic bone lesions were identified in any of the mutant mice by dissection or CT scanning. In addition, individual leg tendons and their muscles could be identified by careful dissection, indicating that the bony expansion was not a result of heterotopic ossification.

Dramatic increases in total bone volume and trabecular bone volume, with almost complete loss of the cortical shell and marrow space, were seen on histomorphometric analysis of femurs from 9-week-old mice. High-magnification images of both 3- and 9-week-old femurs showed a large number of cells with uniform morphology interdigitated between the trabeculi, with many appearing stacked on and near the rough trabecular surface (Fig. 4 *A* and *B*, and see SI Figs. 7 *A–C* and 8 *A* and *B*). Normal bone marrow structure was disrupted, with loss of the normal bone marrow cavity. Bone marrow elements appeared to be scattered in small islands between the trabeculi (SI Fig. 7 *A* and *B*). Red blood cell, white blood cell, and platelet counts in the mutant mice were indistinguishable from WT controls through 9 weeks of age. No sites of extramedullary hematopoiesis were identified by histology of the spleen, liver, or kidney.

qPCR analysis on 9-week-old WT and ColI(2.3)+/Rs1+ bones (Fig. 4 *G* and *H*) showed a moderate increase in osteocalcin expression and a dramatic increase in osterix expression, suggesting a relative increase in osteoblast-lineage cells in the ColI(2.3)+/Rs1+ bone lesions. Immunohistochemistry with an antibody against the FLAG tag on Rs1 identified a significant number of cells within the ColI(2.3)+/Rs1+ bone lesions expressing Rs1 (SI Fig. 7 *D* and *E*). These cells likely represent maturing osteoblasts, based on the known expression patterns of the Col1α-1 2.3-kb promoter fragment (27, 28) and on the presence of abundant osteocalcin in the bone lesions (SI Fig. 7 *F* and *G*). Osterix expression was detected by immunohistochemistry in WT animals (SI Fig. 7 *J* and *K*) only in the trabecular bone at the epiphysis. In contrast, osterix was easily detected throughout the ColI(2.3)+/Rs1+ bone lesions (SI Fig. 7 *L* and *M*). These immunohistochemistry results confirm that many of the uniform cells in the ColI(2.3)+/Rs1+ bone lesions are in the osteoblast lineage. The requirement for different fixation methods precluded us from colocalization of Rs1 with osterix or osteocalcin on these samples.

We used dual fluorochrome labeling to examine the bone formation rate and pattern in 3-week-old (SI Fig. 8 *C* and *D*) and 9-week-old (Fig. 4 *C* and *D*) ColI(2.3)+/Rs1+ mice. The mutant mice showed disordered bone formation, indicated by punctate labeling seen at high magnification, preventing accurate measurement of bone formation rates. Low-magnification images

CELL BIOLOGY

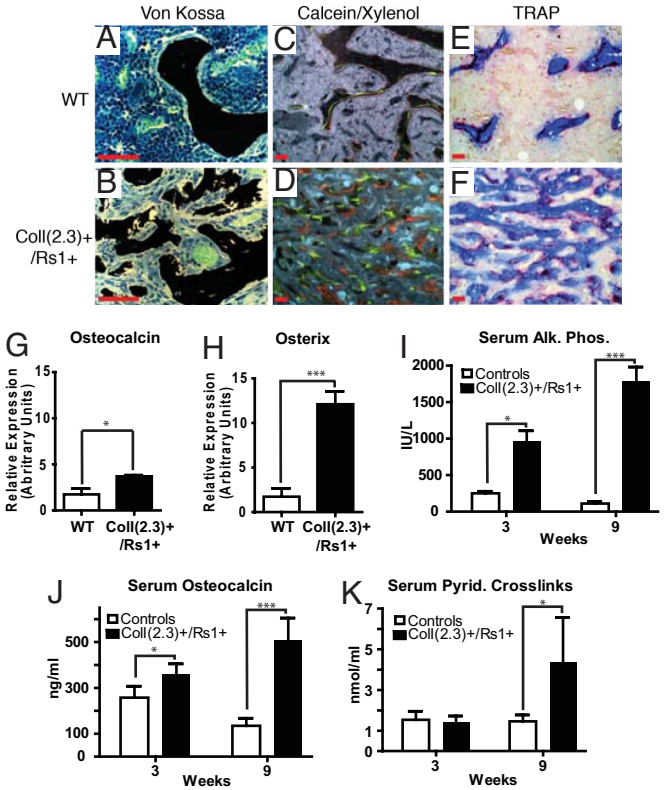

Fig. 4. Bone histomorphometry and serum markers in Rs1-expressing mice. (*A* and *B*) Von Kossa/tetrachrome staining of femurs at 9 weeks of age shows disorganized trabeculi and a population of uniform cells replacing the normal bone marrow cavity in double transgenic mice. (*C* and *D*) Bone-mineral apposition was assessed by dual fluorochrome labeling with calcein (green) and xylenol orange (orange), injected 5 days apart. The disordered growth pattern in the mutant mice prevented accurate measurement of bone formation rates. (*E* and *F*) TRAP staining (red) suggests increased osteoclast activity consistent with the increased bone surface. (Scale bars, 50 μm.) (*G* and *H*) qPCR analysis on mRNA from 9-week-old femurs of WT (n = 3 mice, tested in triplicate) and ColI(2.3)+/Rs1+ (n = 4 mice, tested in triplicate), showing increases in osteocalcin (*G*) and osterix (*H*) expression levels. (*I–K*) Serum markers of bone formation [alkaline phosphatase (*I*) and osteocalcin (*J*)] and bone resorption [pyridinoline cross-links (*K*)] were elevated in double transgenic mice. For all 3-week blood work, n = 5 WT and 5 mutant mice. For 9-week alkaline phosphatase, n = 2 WT and 6 mutants; osteocalcin and pyridinoline levels, n = 3 WT and 8 mutants. Error bars represent ±1 SD. *, $P < 0.05$; ***, $P < 0.0005$ by t test of Rs1-expressing mice vs. control genotypes.

showed several regions of relatively discrete xylenol orange or calcein labeling interspersed with regions labeled with both fluorochromes, suggesting localized regions of high bone turnover. Rapid bone turnover was also suggested by the large number of tartrate-resistant acid phosphatase (TRAP)-positive regions adjacent to the trabeculi within the lesions (Fig. 4 *E* and *F*, and see SI Fig. 8 *E* and *F*), indicating an increase in osteoclast number.

Basic serum parameters were similar in all genotypes in 3-week-old (SI Table 2) and 9-week-old (SI Table 3) mice. In contrast, markers of bone turnover were increased in the affected mice at both ages (Fig. 4 *I–K*). These results, along with the nodular pattern seen on fluorochrome labeling and on cross-sectional CT analysis, suggest that the bony lesions contain regions of extremely high rates of bone formation and turnover consistent with rapid remodeling activity.

We used the tTA system to determine whether expression of Rs1 during the period of rapid bone growth in the first several weeks of life is required for the full effect of Rs1 on bone formation. Rs1 expression was suppressed up to weaning (3 weeks of age) by administration of doxycycline to mothers during pregnancy and lactation. After weaning, pups were maintained on doxycycline-containing food for an additional week and then switched to a doxycycline-free diet to allow Rs1 expression. Longitudinal assessment of these mice did not show a detectable bone phenotype by DEXA BMD, weight, or length measurements through 30 weeks of age (SI Fig. 9). Our results suggest that the dramatic effect of Rs1 on bone accrual requires expression of Rs1 during the first 4–6 weeks of murine life.

Discussion

Our studies demonstrate that osteoblast expression of Rs1, an engineered G_s-coupled RASSL with constitutive G_s activity, induces a dramatic anabolic bone effect that is significantly different from previous models (10–15). The ColI(2.3)+/Rs1+ mice display several unique and unexpected characteristics, including a crucial temporal requirement for Rs1 expression, an unusually large amount of bone mineral accrual, and effects on bone macroarchitecture. Our results add to prior studies (10–15) that support the anabolic role of G_s signaling in osteoblasts by using a model system that controls G_s activation without potential confounding effects from endogenous ligands or nonskeletal PTHR1 activation. In addition, Rs1 basal signaling activity appears to be selective for the G_s pathway, with little or no activation of the G_q pathway. Thus, the lesser effect of constitutively active PTHR1 signaling on bone mass (10) may be attributable to PTHR1-induced activation of additional G protein signaling pathways, including G_i and G_q, that could counteract the anabolic effects of G_s activation. Recent studies lend support to this notion, because osteoblast expression of a constitutively active $G_q\alpha$ (29) or a constitutively active G_i-coupled GPCR (26, 30) leads to decreased trabecular bone. Mice expressing the constitutively active PTHR1 also show expansion of trabecular bone, with delay of bone marrow cavity formation (31); however, the ColI(2.3)+/Rs1+ mice appear to have a more severe phenotype and do not appear to reform a true bone marrow space as they age.

The dramatic loss of cortical bone in the ColI(2.3)+/Rs1+ lesions is reminiscent of that found in primary hyperparathyroidism, in which continuous PTHR1 receptor activation by PTH leads to a decrease in cortical bone mass. Patients with primary hyperparathyroidism show largely unaffected trabecular bone structures (32, 33), which contrasts sharply with the massive increases in trabecular bone seen in the ColI(2.3)+/Rs1+ mice. We speculate that the enhanced expansion of trabecular bone in the ColI(2.3)+/Rs1+ mice may be a result of chronic G_s activation during the prepubertal growth phase and that PTHR1-induced G_i and G_q signaling may be modulated in normal prepubertal growth to allow rapid expansion of the growing skeleton. Furthermore, intermittent administration of recombinant PTH to adult patients leads to an increase in both cortical bone mass and bone strength (34, 35). The differences in response to intermittent vs. chronic PTHR1 activation indicate that basal vs. ligand-induced G_s activity may regulate the balance between cortical and trabecular bone formation.

Our data show that osteoblast-lineage cells in prepubertal mice have an enormous bone-forming capacity. Many clinical conditions affecting bone show age-dependence. Several types of primary skeletal tumors, including osteosarcoma and Ewing's sarcoma, have a higher prevalence in children and adolescents than in adults (36, 37). In addition, older patients (38–41) and older animals (42–44) recover more slowly after certain types of fracture. Recent animal studies in young rats (45), and clinical studies in young children (46), suggest that exercise during childhood can lead to an increase in bone mass that persists with age. The ColI(2.3)+/Rs1+ mice also share features with the polyostotic fibrous dysplasia of McCune–Albright's syndrome, a

predominantly pediatric disease caused by the expression of a constitutively active form of $G_s\alpha$ (47). This sensitivity of early postnatal osteoblasts to G_s activation may provide a cellular explanation for these age-related differences in bone growth and healing.

Stem cell and osteoblast models could be developed to determine the cellular basis of the ColI(2.3)+/Rs1+ phenotype and to further investigate the roles of specific signaling pathways as downstream mediators of Rs1 activity. Direct, controlled regulation of the yet-to-be-identified anabolic target may also be useful for improving fracture healing or surgical repair, as well as for developing potential treatments for skeletal diseases such as fibrous dysplasia (9), osteoblastomas, osteoid sarcomas (48, 49), and osteoblastic bone metastases (50). Our RASSL system will also permit examination of the contributions of both basal G_s signaling activity and ligand-mediated receptor activation. Such studies have exciting implications for revealing new mechanisms for the control of bone formation.

Materials and Methods

Constructs. The WT human 5HT4b receptor cDNA was obtained from W. Kroeze and B. Roth (University of North Carolina, Chapel Hill, NC). The human 5HT4b cDNA coding region was amplified by PCR cloning (primers are listed in SI Table 1 *A*) to introduce flanking NotI cloning sites. The 5HT4b PCR fragment was used to replace the entire 5HT2c receptor coding region via the NotI sites of the pUNIV-5HT2c-INI plasmid (also kindly provided by W. Kroeze and B. Roth) in frame with the existing signal peptide and the FLAG epitope (DKYDDDDA). The 5HT4-D100A mutation was introduced by using the QuikChange site-directed mutagenesis kit (Stratagene) and the sense primer (SI Table 1*B*) to generate the Rs1 receptor in the plasmid pUNIV-SIG-5HTR4D100A (Addgene plasmid database no. 16312). All constructs were verified by sequencing. The pUNIV-SIG-5HTR4D100A plasmid was used directly for expression and signaling analysis in HEK293 cells.

cAMP Production and Calcium Mobilization Assays. These assays were performed as described in *SI Materials and Methods*, using the Hi-Range HTRF kit (CisBio) and FLIPR Calcium4 flurometric plate reader assay (Molecular Devices).

Generation of Mice. All transgenic mouse studies were approved by, and performed in accordance with, the Institutional Animal Care and Use Committee and the Laboratory Animal Research Center at the University of California, San Francisco.

TetO-Rs1 Construct and Transgenic Mouse. To regulate expression of Rs1 with tetracycline or doxycycline, the Rs1 cDNA construct was cloned into the pUHG10.3 vector (51) containing the TetO promoter, β-globin intron, and pA sites (pUHG10.3 TetO-Rs1; Addgene plasmid no. 16313). A 3-kb XhoI/SapI fragment was isolated by restriction digestion and used to generate the TetO-Rs1 transgenic mice by pronuclear injection into FVBN oocytes (Gladstone Transgenic Core). Chimeric mice were backcrossed and maintained on a FVBN background. Seven chimeric mice were identified, and three lines (designated B, C, and G) demonstrated germ-line transmission by PCR genotyping (SI Table 1 *C* and *D*). Because the three distinct lines showed no phenotypic differences, all studies presented here use the TetO-Rs1 line G. These mice have been deposited in the Mutant Mouse Regional Resource Centers (MMRRC) database [accession no. 029992, FVB/N-Tg(TetO-HTR4*D100A)]. A second line (line B) with slightly lower Rs1 expression levels in the bone has also been deposited [MMRRC accession no. 029993 FVB/N-Tg(TetO-HTR4*D100A)].

Generation of ColI(2.3)-tTA/TetO-Rs1 Mice. The ColI(2.3)-tTA/TetO-Rs1 double transgenic mice were generated by heterozygote crosses of mice carrying the TetO-Rs1 transgene with mice carrying the ColI(2.3)-tTA transgene (line 139) (26), to generate the experimental double transgenic genotype and the three control genotypes (see SI Fig. 5*A* for mating strategy). Transgene expression was suppressed with doxycycline-impregnated mouse chow (DoxDiet 200 mg/kg; BioServ). Transgene expression was activated by switching the mice to regular mouse chow without doxycycline at 4 weeks of age (LabDiet 5053; PMI Nutrition). Full transgene expression was expected to occur within 2 weeks after doxycycline withdrawal, based on prior data (20). qPCR from whole femurs of 6-week-old adult mice showed that Rs1 expression was induced ≈4- to 80-fold above that of age-matched ColI(2.3)+/Rs1+ mice that were chronically maintained on doxycycline (SI Fig. 5*D*). qPCR and serum analyses were carried out as described in *SI Materials and Methods*.

Bone Imaging. Mice identified for bone densitometry (DEXA) scans were anesthetized with inhaled isofluorane (1.5–2% in oxygen) and scanned at predetermined time points using a Lunar PIXImus2 (GE Lunar). Whole-mouse and femur CT scans were performed on euthanized animals with a vivaCT40 microCT scanning system (Scanco), as described in *SI Materials and Methods*.

Histology and Immunohistochemistry. Mice identified for histomorphometry were injected with calcein (Sigma–Aldrich) at day −7 and with xylenol orange (Sigma–Aldrich) at day −2 before harvesting. Isolated bone samples were processed as described in *SI Materials and Methods*.

ACKNOWLEDGMENTS. We thank Sharon Chung, Matthew Spindler, Alyssa Louie, Robert Farese, Eileen Shore, Andrew Horvai, Richard Schneider, Wenhan Chang, Yong-mei Wang, Grant Yang, Gary Howard, and Stephen Ordway for technical assistance and valuable discussions. This work was supported in part by National Institutes of Health (NIH) Fellowship Training Grant 2T32DK07418-26 and California Institute of Regenerative Medicine (CIRM)/J. David Gladstone Institute CIRM Fellowship Program Grant T2-00003 (to E.C.H.); the San Francisco Veterans Affairs Research Enhancement Awards Program (D. D. Bikle, Program Director); NIH R01 Grants HL60664-07 (to B.R.C.) and DK072071 (to R.A.N.); American Heart Association Predoctoral Fellowship Program Grant 0415005Y (to W.C.C.), and the Veterans Affairs Merit Review Program (B.P.H. and R.A.N.). The J. David Gladstone Institutes received support from National Center for Research Resources Grant RR18928-01. R.A.N. and B.P.H. are Senior Research Career Scientists of the Department of Veterans Affairs.

1. Aubin JE, Lian JB, Stein GS (2006) Bone formation: Maturation and functional activities of osteoblast lineage cells. *Primer on the Metabolic Bone Diseases and Disorders of Mineral Metabolism*, ed Favus MJ (Am Soc for Bone and Mineral Res, Washington, DC), pp 20–29.
2. National Osteoporosis Foundation (2002) *America's Bone Health: The State of Osteoporosis and Low Bone Mass in Our Nation* (Natl Osteoporosis Found, Washington, DC).
3. American Academy of Orthopaedic Surgeons (2007) *Emergency Room Visits for Fractures.* Available at www.aaos.org/Research/stats/ER%20Visits%20for%20Fracture.pdf.
4. Dobnig H, Turner RT (1997) The effects of programmed administration of human parathyroid hormone fragment (1–34) on bone histomorphometry and serum chemistry in rats. *Endocrinology* 138:4607–4612.
5. Gether U (2000) Uncovering molecular mechanisms involved in activation of G protein-coupled receptors. *Endocrinol Rev* 21:90–113.
6. Weinstein LS, *et al.* (2004) Minireview: GNAS: normal and abnormal functions. *Endocrinology* 145:5459–5464.
7. Sakamoto A, *et al.* (2005) Chondrocyte-specific knockout of the G protein G(s)alpha leads to epiphyseal and growth plate abnormalities and ectopic chondrocyte formation. *J Bone Miner Res* 20:663–671.
8. Sakamoto A, *et al.* (2005) Deficiency of the G-protein alpha-subunit G(s)alpha in osteoblasts leads to differential effects on trabecular and cortical bone. *J Biol Chem* 280:21369–21375.
9. Weinstein LS (2006) G(s) alpha mutations in fibrous dysplasia and McCune–Albright syndrome. *J Bone Miner Res* 21(Suppl 2):P120–P124.
10. Calvi LM, *et al.* (2001) Activated parathyroid hormone/parathyroid hormone-related protein receptor in osteoblastic cells differentially affects cortical and trabecular bone. *J Clin Invest* 107:277–286.
11. Guo J, *et al.* (2002) The PTH/PTHrP receptor can delay chondrocyte hypertrophy in vivo without activating phospholipase C. *Dev Cell* 3:183–194.
12. Armamento-Villareal R, *et al.* (1997) An intact N terminus is required for the anabolic action of parathyroid hormone on adult female rats. *J Bone Miner Res* 12:384–392.
13. Hilliker S, *et al.* (1996) Truncation of the amino terminus of PTH alters its anabolic activity on bone *in vivo*. *Bone* 19:469–477.
14. Rixon RH, *et al.* (1994) Parathyroid hormone fragments may stimulate bone growth in ovariectomized rats by activating adenylyl cyclase. *J Bone Miner Res* 9:1179–1189.
15. Whitfield JF, *et al.* (1996) Stimulation of the growth of femoral trabecular bone in ovariectomized rats by the novel parathyroid hormone fragment, hPTH-(1–31)NH2 (Ostabolin). *Calcif Tissue Intl* 58:81–87.
16. Coward P, *et al.* (1998) Controlling signaling with a specifically designed G_i-coupled receptor. *Proc Natl Acad Sci USA* 95:352–357.
17. Armbruster BN, *et al.* (2007) Evolving the lock to fit the key to create a family of G protein-coupled receptors potently activated by an inert ligand. *Proc Natl Acad Sci USA* 104:5163–5168.
18. Scearce-Levie K, Lieberman MD, Elliott HH, Conklin BR (2005) Engineered G protein coupled receptors reveal independent regulation of internalization, desensitization and acute signaling. *BMC Biol* 3:3.
19. Zhao GQ, *et al.* (2003) The receptors for mammalian sweet and umami taste. *Cell* 115:255–266.

20. Redfern CH, *et al.* (1999) Conditional expression and signaling of a specifically designed G_i-coupled receptor in transgenic mice. *Nat Biotechnol* 17:165–169.
21. Sweger EJ, *et al.* (2007) Development of hydrocephalus in mice expressing the G(i)-coupled GPCR Ro1 RASSL receptor in astrocytes. *J Neurosci* 27:2309–2317.
22. Redfern CH, *et al.* (2000) Conditional expression of a Gi-coupled receptor causes ventricular conduction delay and a lethal cardiomyopathy. *Proc Natl Acad Sci USA* 97:4826–4831.
23. Claeysen S, *et al.* (2003) A single mutation in the 5-HT4 receptor (5-HT4-R D100(3.32)A) generates a Gs-coupled receptor activated exclusively by synthetic ligands (RASSL). *J Biol Chem* 278:699–702.
24. Furth PA, *et al.* (1994) Temporal control of gene expression in transgenic mice by a tetracycline-responsive promoter. *Proc Natl Acad Sci USA* 91:9302–9306.
25. Kistner A, *et al.* (1996) Doxycycline-mediated quantitative and tissue-specific control of gene expression in transgenic mice. *Proc Natl Acad Sci USA* 93:10933–10938.
26. Peng JT, *et al.* (November 29, 2007) Conditional expression of a Gi-coupled receptor in osteoblasts results in trabecular osteopenia. *Endocrinology*, 10.1210/en.2007-0235.
27. Dacquin R, Starbuck M, Schinke T, Karsenty G (2002) Mouse alpha1(I)-collagen promoter is the best known promoter to drive efficient Cre recombinase expression in osteoblast. *Dev Dyn* 224:245–251.
28. Dacic S, *et al.* (2001) Col1a1-driven transgenic markers of osteoblast lineage progression. *J Bone Miner Res* 16:1228–1236.
29. Ogata N, *et al.* (2007) Continuous activation of $G\alpha_q$ in osteoblasts results in osteopenia through impaired osteoblast differentiation. *J Biol Chem* 282:35757–35764.
30. Peng JT, *et al.* (2006) Osteopenia produced by expression of a Gi-activating receptor in osteoblasts. *J Bone Miner Res* 21:S99, Abstract F222.
31. Kuznetsov SA, *et al.* (2004) The interplay of osteogenesis and hematopoiesis: Expression of a constitutively active PTH/PTHrP receptor in osteogenic cells perturbs the establishment of hematopoiesis in bone and of skeletal stem cells in the bone marrow. *J Cell Biol* 167:1113–1122.
32. Charopoulos I, *et al.* (2006) Effect of primary hyperparathyroidism on volumetric bone mineral density and bone geometry assessed by peripheral quantitative computed tomography in postmenopausal women. *J Clin Endocrinol Metab* 91:1748–1753.
33. Dempster DW, *et al.* (2007) Preserved three-dimensional cancellous bone structure in mild primary hyperparathyroidism. *Bone* 41:19–24.
34. Body JJ, *et al.* (2002) A randomized double-blind trial to compare the efficacy of teriparatide [recombinant human parathyroid hormone (1–34)] with alendronate in postmenopausal women with osteoporosis. *J Clin Endocrinol Metab* 87:4528–4535.
35. Reeve J, *et al.* (1980) Anabolic effect of human parathyroid hormone fragment on trabecular bone in involutional osteoporosis: A multicentre trial. *Br Med J* 280:1340–1344.
36. Miller RW, Boice JD, Jr, Curtis RE (2006) Bone cancer. *Cancer Epidemiology and Prevention*, eds Schottenfeld D, Fraumeni JF (Oxford Univ Press, Oxford), pp 946–958.
37. Wu XC, *et al.* (2003) Cancer incidence in adolescents and young adults in the United States, 1992–1997. *J Adolesc Health* 32:405–415.
38. Claes L, *et al.* (2002) Monitoring and healing analysis of 100 tibial shaft fractures. *Langenbecks Arch Surg* 387:146–152.
39. Nieminen S, Nurmi M, Satokari K (1981) Healing of femoral neck fractures: Influence of fracture reduction and age. *Ann Chir Gynaecol* 70:26–31.
40. Nilsson BE, Edwards P (1969) Age and fracture healing: A statistical analysis of 418 cases of tibial shaft fractures. *Geriatrics* 24:112–117.
41. Skak SV, Jensen TT (1988) Femoral shaft fracture in 265 children. Log-normal correlation with age of speed of healing. *Acta Orthop Scand* 59:704–707.
42. Lu C, *et al.* (2005) Cellular basis for age-related changes in fracture repair. *J Orthop Res* 23:1300–1307.
43. Meyer RA, Jr, *et al.* (2006) Young, adult, and old rats have similar changes in mRNA expression of many skeletal genes after fracture despite delayed healing with age. *J Orthop Res* 24:1933–1944.
44. Tonna EA, Cronkite EP (1962) Changes in the skeletal cell proliferative response to trauma concomitant with aging. *J Bone Jt Surg Am Vol* 44:1557–1568.
45. Warden SJ, *et al.* (2007) Exercise when young provides lifelong benefits to bone structure and strength. *J Bone Miner Res* 22:251–259.
46. MacKelvie KJ, *et al.* (2003) A school-based exercise intervention elicits substantial bone health benefits: A 2-year randomized controlled trial in girls. *Pediatrics* 112:e447–e452.
47. Weinstein LS, *et al.* (1991) Activating mutations of the stimulatory G protein in the McCune–Albright syndrome. *N Engl J Med* 325:1688–1695.
48. Bahk WJ, Mirra JM (2004) Pseudoanaplastic tumors of bone. *Skeletal Radiol* 33:641–648.
49. Kyriakos M, *et al.* (2007) Osteoblastomatosis of bone. A benign, multifocal osteoblastic lesion, distinct from osteoid osteoma and osteoblastoma, radiologically simulating a vascular tumor. *Skeletal Radiol* 36:237–247.
50. Hall CL, Keller ET (2006) The role of Wnts in bone metastases. *Cancer Metastasis Rev* 25:551–558.
51. Gossen M, Bujard H (1992) Tight control of gene expression in mammalian cells by tetracycline-responsive promoters. *Proc Natl Acad Sci USA* 89:5547–5551.